ORIGINAL PAPER

Optimization of Microwave Presplitting Iron Ore to Improve Mechanical Mining Efficiency

Feng Lin[1,2] · Xia-ting Feng[1,2] · Shi-ping Li[1,2] · Jiu-yu Zhang[1,2] · Xiang-xin Su[1,2] · Tian-yang Tong[1,2]

Abstract

Optimizing the microwave parameters adopted in microwave-assisted mechanical mining is of great significance to improving the efficiency of the deep resource development. The effects of varying the type of microwave antenna, microwave power, and working distance on the reflection coefficient and heating characteristics of Sishanling iron ore were studied. The optimized microwave operating parameters were proposed, and microwave irradiation and mechanical cutting tests were then carried out on the ore samples under true triaxial stress conditions to verify the feasibility of the optimized parameters. The results show that the ore's reflection coefficient increased at first and then decreased as the working distance (2–8 cm) was increased. The reflection coefficient increased as the microwave power was increased. Compared with other distances, the temperature and temperature gradient of the irradiated surfaces of samples were maximized when the working distance was 2 cm. The optimum microwave parameters of iron ore were: a microwave antenna format of horn antenna/standard waveguide antenna, a working distance of 2 cm. Under true triaxial stress conditions, samples suffered no macroscopic damage when irradiated for 300 s at a working distance of 8 cm. When the working distance was reduced to 2 cm, however, samples broke apart after just 10 s (failure mainly taking the form of intermittent spalling). Arcing readily occurred under true triaxial stress conditions when the working distance was 2 cm. This phenomenon occurred on the irradiated surface of the sample and the baffle of the antenna could also be ignited. Ways of optimizing the antenna were put forward and discussed.

Highlights

- The influence of microwave antenna type, microwave power and working distance on reflection coefficient and heating characteristics of Sishanling iron ore was studied.
- The influence of optimized working distance on microwave cracking effect of ore under true triaxial stress was studied.
- The optimization scheme of microwave antenna was proposed based on the arc phenomenon of ore.

✉ Xia-ting Feng
  fengxiating@mail.neu.edu.cn

1 Key Laboratory of Ministry of Education on Safe Mining of Deep Metal Mines, Northeastern University, Shenyang 110819, China

2 Key Laboratory of Liaoning Province on Deep Engineering and Intelligent Technology, Northeastern University, Shenyang 110819, China

1 Introduction

Rock breaking engineering (e.g. tunneling and mining) is gradually migrating to greater depths. Therefore, the traditional excavation method—blasting—is becoming less able to meet safety and environmental protection requirements (Natanzi and Laefer 2015; Hartlieb et al. 2017). As a result, non-explosive excavation techniques are becoming more important (Armaghani et al. 2021; Kahraman et al. 2020). At present, methods involving mechanical rock fragmentation have proved to be the most economical approach to dealing with this issue. However, extremely hard rocks are being encountered more often which greatly reduces the excavation speed and causes serious wear to the mechanical

excavation tools employed (Liu and Liang 2000; Entacher et al. 2014; Rostami 2016). One approach to solving this problem is to pretreat the rock to weaken its mechanical properties before mechanical excavation is carried out. Such an approach can reduce the amount of energy consumed and reduce the wear suffered by the mechanical cutting tools employed. Pretreatment methods currently include breaking the rock using water jets, lasers, and microwaves (Montross et al. 1999; Ciccu and Grosso 2014; Lin et al. 2022a). The use of microwaves has great prospects and enjoys certain advantages compared to other methods (a large volume of rock can be quickly heated, there is no danger to the environment, the technique is easy to use, and machinery can be combined with microwave, etc.). The essence of damage is that the temperature of absorbing minerals rises, which leads to rock deformation caused by uneven thermal expansion of mineral particles and the change of mineral composition at high temperature.

The concept of microwave-assisted rock drilling was first put forward in the 1960s (Maurer 1968). Since then, a large number of studies have been carried out on microwave-assisted grinding and excavation. It has thus been shown that microwave treatment significantly reduces the strength of the ore, makes it much easier to grind, and improves the degree of dissociation of the ore (Kingman et al. 2000; Amankwah et al. 2005; Lin et al. 2021). The strength of even hard rocks, e.g. basalt and granite, is greatly reduced after microwave treatment (Toifl et al. 2015; Deyab et al. 2021) which makes it significantly easier to drill and cut them (Jerby et al. 2002; Hartlieb et al. 2017; Shepel et al. 2018).

Although microwaves can have a significant breaking effect on rock, some scholars (Haque 1999) have suggested that their use is uneconomical. Therefore, improving the efficiency of the microwave is of great significance to the successful industrial application of microwave-assisted excavation. This means that more research is needed in this field (from equipment research and development to parameter optimization). In the early days, the microwave equipment used in the rock treatment experiments took the form of a closed microwave cavity (Kingman et al. 2004; Peinsitt et al. 2010; Zheng et al. 2017). However, such an arrangement is hardly appropriate in the context of a mining face which is exposed to the air on one side only. Thus, open microwave-fracturing equipment for hard rock was later developed (Lu et al. 2019). In addition, considering that high stress is generally encountered in deep tunnels and mines, it is important to note that Feng et al. (2021) have also developed a true triaxial hard rock microwave fracturing device.

Microwave-assisted excavation involves various parameters that need to be optimized. These include the microwave power employed, irradiation time, distance between the irradiated surface and antenna ('working distance'), and the size of the antenna. In general, the higher the microwave power and the longer the irradiation time, the better the microwave cracking effect produced in the rock (Kahraman et al. 2020; Zheng et al. 2020). For a fixed amount of output microwave energy, the higher the power and shorter the irradiation time, the greater the temperature rise in the rock and the better the generation of fractures (Kingman et al. 1999; Lester and Kingman 2004; Huang et al. 2018). In this context, it has been found that a single mode applicator can produce a higher power density (Hassani and Nekoovaght 2011). Hassani et al. (2016, 2020) conducted microwave experiments on basalt and investigated the effect on heating efficiency of changing sample shape and antenna position. Teimoori and Cooper (2021) have suggested that a combination of high microwave power and small antenna–sample distance provides the best energy efficiency. Antenna selection is another important factor affecting the efficiency of the microwave–rock interaction. Common types of antennae include horn antennae, standard waveguide antennae, and convergent waveguide antennae (Hartlieb and Grafe 2017;; Lu et al. 2019; Ma et al. 2021). Convergent waveguide antennae enhance the power density at the antenna aperture (compared to horn antennae) by reducing the size of its E-plane. On the other hand, they have poor directivity and smaller effective working distance. Ma et al. (2021, 2022) recently used a convergent antenna and low-power microwave source to irradiate rocks. It was found that the heating and cracking effects were inversely proportional to both the size of the antenna and the working distance.

The improper microwave parameters employed may lead to excessive reflection of microwaves which can damage the equipment, especially if the microwave equipment is operating at high power. However, little research has been carried out on the reflection of microwaves from the rock. In addition, when open microwave equipment was used in previous studies, most of the research objects were unstressed rock samples. It is thus not clear what additional phenomena might occur when the target ores experience true triaxial stress, as might well be the case in the field.

In this work, Sishanling iron ore was used as the research object. First, the effects of varying different microwave parameters were studied under stress-free conditions (microwave antenna type, microwave power, and working distance). More specifically, the reflection coefficient and heating characteristics of the ore were explored. The optimal microwave parameters were thus obtained. Then, microwave irradiation and mechanical cutting tests were carried out under true triaxial stress conditions to verify the rationality of these parameters. Finally, the optimization of the antenna was discussed. This study provides useful guidance for the

design and application of microwave-assisted mechanical mining equipment.

2 Experimental Methodology

2.1 Experimental Equipment

A true triaxial system (Fig. 1a) was employed to perform tests on the microwave-treated iron ore samples (Feng et al. 2021). The system includes a loading system, microwave system, and monitoring system. The loading system is configured so that loads can be applied to five sides of the sample (so one side is unloaded). The free side is used to apply microwaves to the surface of the sample thus simulating the on-site irradiation process. The loading system generates different principal stresses in three mutually-perpendicular directions, yielding a maximum load of 5000 kN.

The microwave system provides 2.45 GHz microwave radiation at a maximum power of 15 kW. A single TE10 microwave mode was employed in our experiments. Three different antenna types were used (Fig. 1c): a horn antenna ('antenna 1'), an essentially standard waveguide antenna ('antenna 2'), and a convergent waveguide antenna ('antenna 3'). Mica baffles were fixed to the output ends of the antennae. These baffles are transparent to the microwaves and have high temperature resistance. They are used to prevent any ore particles from breaking free from the samples during the microwave irradiation process and falling into the antennae.

A hard rock true triaxial dual-mode mechanical cutting system (Fig. 1b) was used to cut the ore samples (Feng et al. 2022). The system effectively simulates the act of using a tunnel boring machine to excavate and mechanically mine ore in the high stress conditions usually encountered deep underground. The maximum permitted working pressure of the oil in the hydraulic transmission cylinder was 500 kN, the maximum speed of the cutter head was 10 rad/min, and the diameter of the cutter head used was 360 mm.

2.2 Sample Preparation

The iron ore used in the study was sourced from Benxi, China. The main minerals in the ore, quartz (40–45%) and magnetite (45–50%), were distributed in bands. The bulk ore was processed into cubes of side 200 mm. Samples with similar densities and wave velocities were selected for

(a)   (b)

(c)
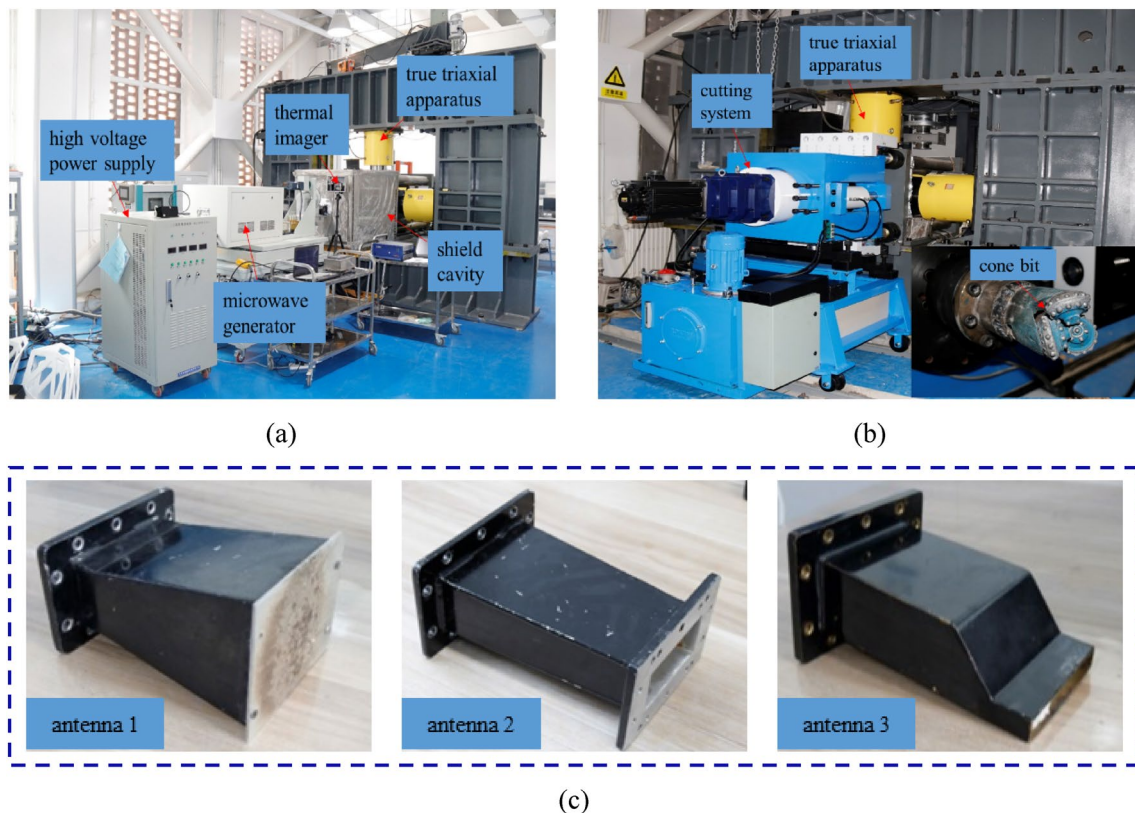
Fig. 1 Various aspects of the testing equipment used: **a** the true triaxial system used to test the microwave-treated rocks (Feng et al. 2021); **b** the cutting equipment (Feng et al. 2022); **c** the antennae used in the tests

the tests: the average density of the samples corresponds to 3358 kg/m^3 and the average wave velocities measured were 6418 m/s (parallel to the bedding plane) and 4653 m/s (perpendicular to the bedding plane).

2.3 Experimental Setup

Considering the limited number of samples available, tests were carried out under stress-free conditions to investigate the relationship between multiple factors and the reflection coefficient. The ore samples were irradiated with microwaves, cooled, and then reused. A lot of attempts were made before the formal test, the ore sample is irradiated by microwave with a certain parameter. After cooling, it is irradiated by microwave with the same microwave parameters. It can be found that when the microwave parameters are the same, the temperature (average temperature, maximum temperature and infrared temperature distribution characteristics) obtained after repeated irradiation are basically the same as the reflection coefficient. Therefore, the reuse of ore samples under stress-free conditions did not affect their heating and reflection performance. The parameter settings used in these formal tests are shown in Table 1. The maximum power used with antenna 3 is limited to 6 kW based on the equipment manufacturer's advice. If the working distance used in the field is too small, the antenna may collide with the rock mass as it moves. Therefore, the working distance is confined to the range 2–8 cm.

The results of the stress-free tests allow the optimal microwave parameters to be determined. The effectiveness of these optimal parameters under more realistic (true triaxial stress) conditions was then evaluated by performing microwave cracking and cutting tests on iron ore samples subjected to true triaxial stress. Experiments were carried out in two groups: one using the optimal parameters and the other using a control set of parameters. The settings used in these true triaxial stress experiments are shown in Table 2.

2.4 Experimental Steps

1. Measurement of Reflection Coefficient and Temperature under Stress-Free Conditions

The purpose of this step is to study the influence of microwave parameters (antenna type, microwave power and working distance) on the temperature-rising characteristics and reflection performance of ore, so as to obtain the optimized microwave parameters. Stress-free ore was irradiated with microwave radiation and the reflection coefficient from the ore recorded every 5 s. The average of the recorded values was then calculated. The reflection coefficient is monitored by a microwave reflection power meter connected to the coupler (Fig. 2a).

Before each experiment, under the condition of low power (2 kW), the reflection coefficient is adjusted to the lowest by using a three-screw impedance tuner, and the experiment is started after the ore is cooled. When the reflection coefficient is a, it means that the incident power is 100*a W. After microwave irradiation, an infrared thermal imager was immediately used to photograph the irradiated surface and hence determine the temperature of the sample. The experiment was continued until the ore cools to room temperature.

2. Microwave Irradiation of Samples Subjected to True Triaxial Stress

To verify the feasibility of the optimized parameters, the microwave irradiation experiment was carried out with the optimized parameters under the true triaxial stress. The distance between the antenna and sample surface to be irradiated was first adjusted to the required value and the electromagnetic shields put into place. Then, the loads in the X-, Y-, and Z-directions were increased at the same time until the required stress conditions were produced (the loading

Table 1 Parameters used in the reflection tests on stress-free ore samples

Antenna type	Section size of antenna (mm^2)	Microwave power (kW)	Heating time (s)	Working distance (cm)
1	109.22×109.22	3, 6, 9, 12, 15	30	2, 4, 6, 8
2	86.36×43.18			
3	109.22×13.65	3, 4, 5, 6		

Table 2 Microwave and cutting parameters used in the tests on ore subjected to true triaxial stress

Antenna type	Microwave power (kW)	Heating time (s)	Working distance (cm)	σ_1–σ_2–σ_3 (MPa)	Drill speed (rad/min)	Cutting time (min)
1	15	30	2	30–20–10	5	20
		300	8			

Fig. 2 **a** Measurement of reflection coefficient and temperature under stress-free condition; **b** schematic diagram showing the coordinate system used and loads applied to the samples; **c** layout of the wave velocity measuring points of ore under the combined action of true triaxial stress and microwave; **d** cutting test of ore under the combined action of true triaxial stress and microwave

(a)

(b)

(c)

(d)
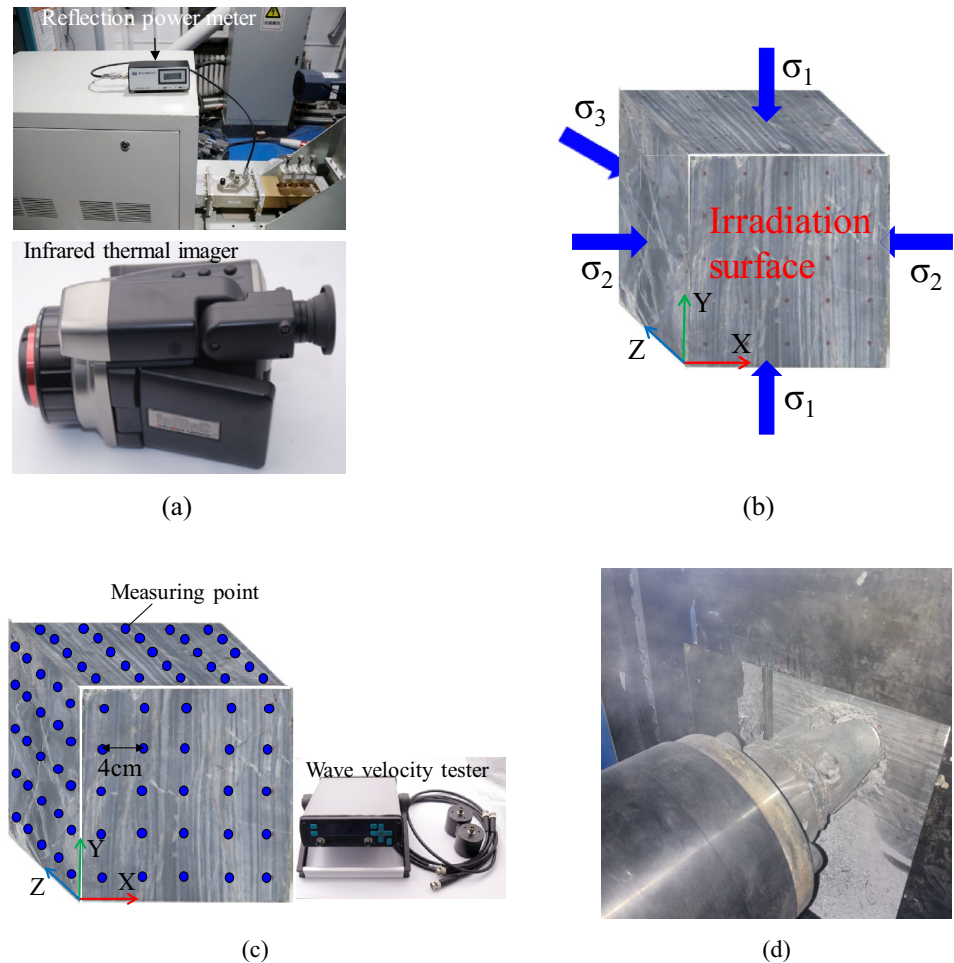
coordinates are shown in Fig. 2b). Loading rates of 2, 2, and 1 kN/s, were used in the three directions, respectively. At the same time, the microwave and acoustic emission (AE) monitoring equipment was turned on with the AE amplitude set to 40 dB. After the microwave irradiation process had been completed, the AE system was turned off. Unloading was first carried out in the Z-direction and then in the X- and Y-directions.

3. Wave Velocity Tests After Microwave Irradiation

The wave velocities in the ore samples were measured before and after microwave irradiation. Measurements were taken at 25 test points on each surface (as shown in Fig. 2c, the distance between adjacent test points is 4 cm). The coupling agent is used in the whole process of wave velocity testing. After using the coupling agent, the wave velocity probe is closely attached to the ore surface to measure the wave velocity. In addition, for the measuring points of the peeling area, the depth of the peeling area is measured, and the depth of the peeling area is removed when calculating the wave velocity

of the peeling area after microwave. Three measurements were made at each point and the results averaged.

4. Mechanical Cutting Tests

Samples were subjected to loads of 100, 100, and 70 kN in the X-, Y-, and Z-directions, respectively (applied at loading rates of 2, 2, and 1 kN/s, respectively). The cutting tool used was a cone bit with a diameter of 98 mm (Fig. 2d). During cutting, an axial thrust of 50 kN was applied while the bit rotated at a speed of 5 rad/min. Cutting was carried out for 20 min.

3 Results and Analysis

3.1 Microwave Reflection Coefficients

Figure 3 shows the average reflection coefficients measured for the samples. It is immediately apparent that the reflection coefficients increase at first as the working distance is increased and then decrease again. The largest reflection
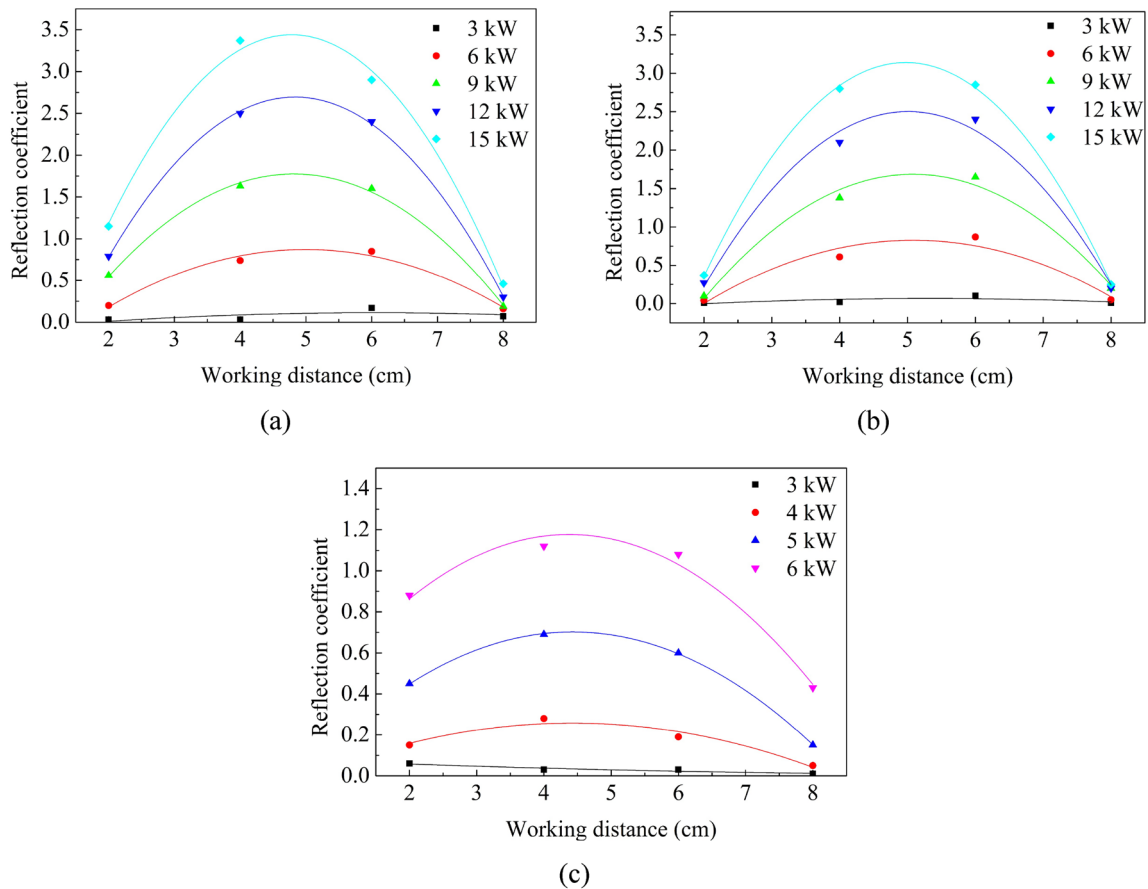
Fig. 3 Variation of the reflection coefficients of the samples with working distance for: **a** antenna 1, **b** antenna 2, and **c** antenna 3

coefficients occur when the working distance is 4–6 cm. Figure 3 also shows that the working distance has a significant effect on the reflection coefficient. Take antenna 1 as an example. When the microwave power is 15 kW, the reflection coefficient is 3.37 when the working distance is 4 cm. When the working distance is reduced to 2 cm, however, the reflection coefficient is reduced to 1.15 (a decrease of 66%). Furthermore, the higher the microwave power, the stronger the effect of working distance on reflection coefficient. For example, when the working distance is reduced from 4 to 2 cm, the reflection coefficient is reduced by 0.01 (3 kW) and 2.22 (15 kW).

The reflection coefficients are replotted in Fig. 4 to highlight the variation with microwave power. Clearly, the reflection coefficients increase approximately linearly as the microwave power is increased (regardless of which antenna is used). Furthermore, the reflection coefficients are essentially the same when the working distance is 4 cm and 6 cm.

Let K be the function whose value corresponds to the slopes of the reflection coefficient vs. microwave power curves (so K is also a function of the working distance and microwave power). Figure 5 shows how K varies as the working distance is varied. As can be seen, for a particular working distance, the K value corresponding to antenna 3 is significantly larger than those of the other two antennae (and the antenna 1 and antenna 2 values are very similar). In addition, the K value first increases and then decreases as the working distance increases. The largest K value is 0.368 which occurs when the working distance is 4 cm.

Here, taking antenna 1 as a standard, an attempt is made to establish a relationship between input power, working distance and reflected power. The reflection coefficients measured using the Sishanling iron ore were subjected to a binary-linear fitting process to yield an empirical expression of the form:

$$P_{Rs} = -4.77 + 0.25P + 1.98d - 0.013Pd - 0.001P^2 \\ - 0.19d^2 \ (R^2 = 0.894), \tag{1}$$
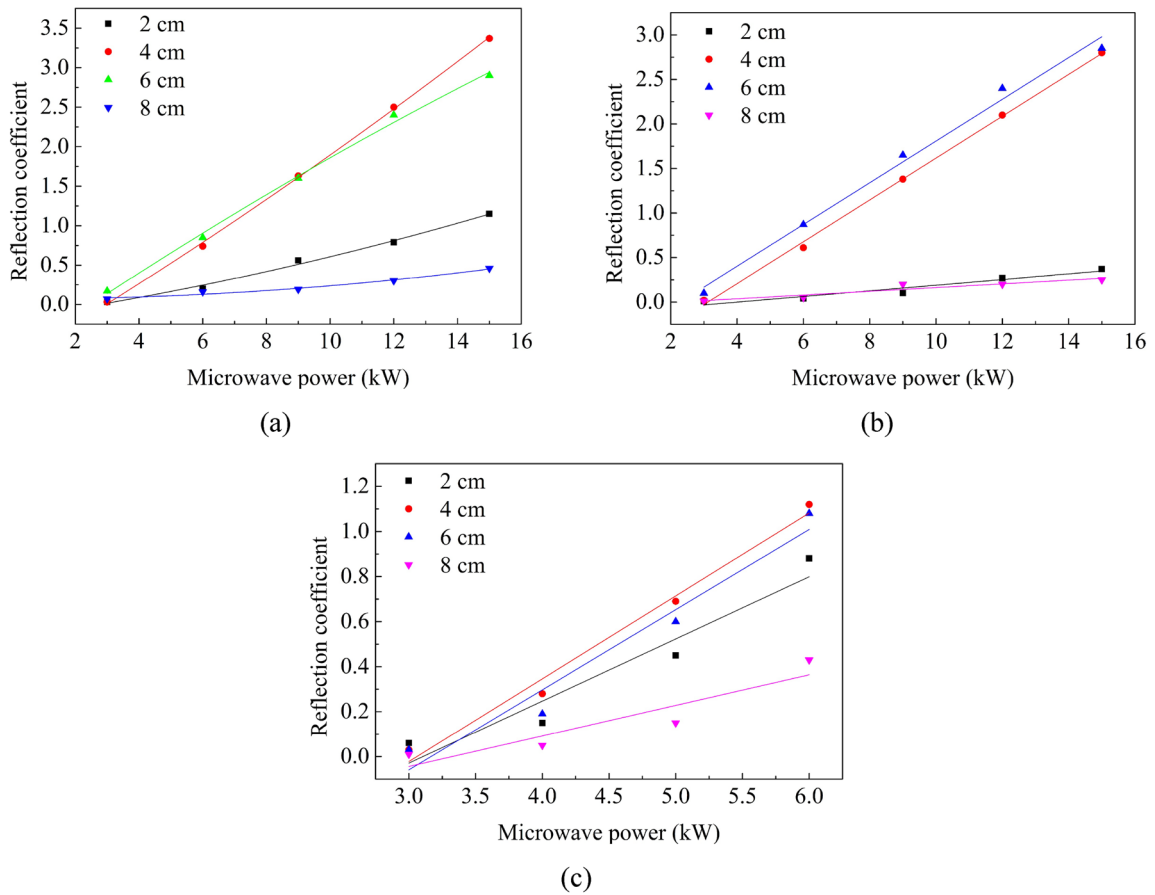
(a)

(b)

(c)

Fig. 4 Variation of the reflection coefficients of the samples with microwave power for: **a** antenna 1, **b** antenna 2, and **c** antenna 3
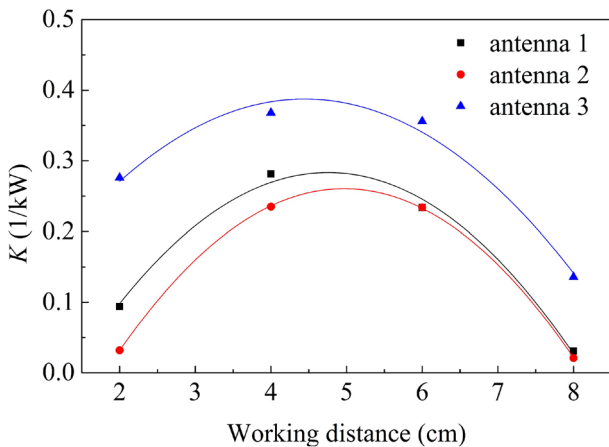

Fig. 5 Variation of the K value of the reflection coefficient of the ore sample with working distance
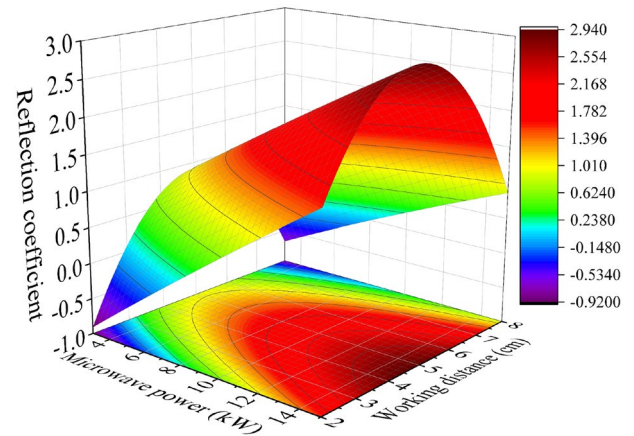

Fig. 6 Surface and contour plots of the reflection coefficient function

where P_{Rs} is the reflection coefficient (when the reflection coefficient P_{Rs} is the value a, it means that the reflection power is 100*a Watts), P (kW) is the input microwave power

($8 \leq P \leq 15$), and d (cm) is the working distance ($2 \leq d \leq 8$). Therefore, the formula can be used to predict the reflection coefficient of Sishanling iron ore within the above range of input power and working distance. Figure 6 presents a
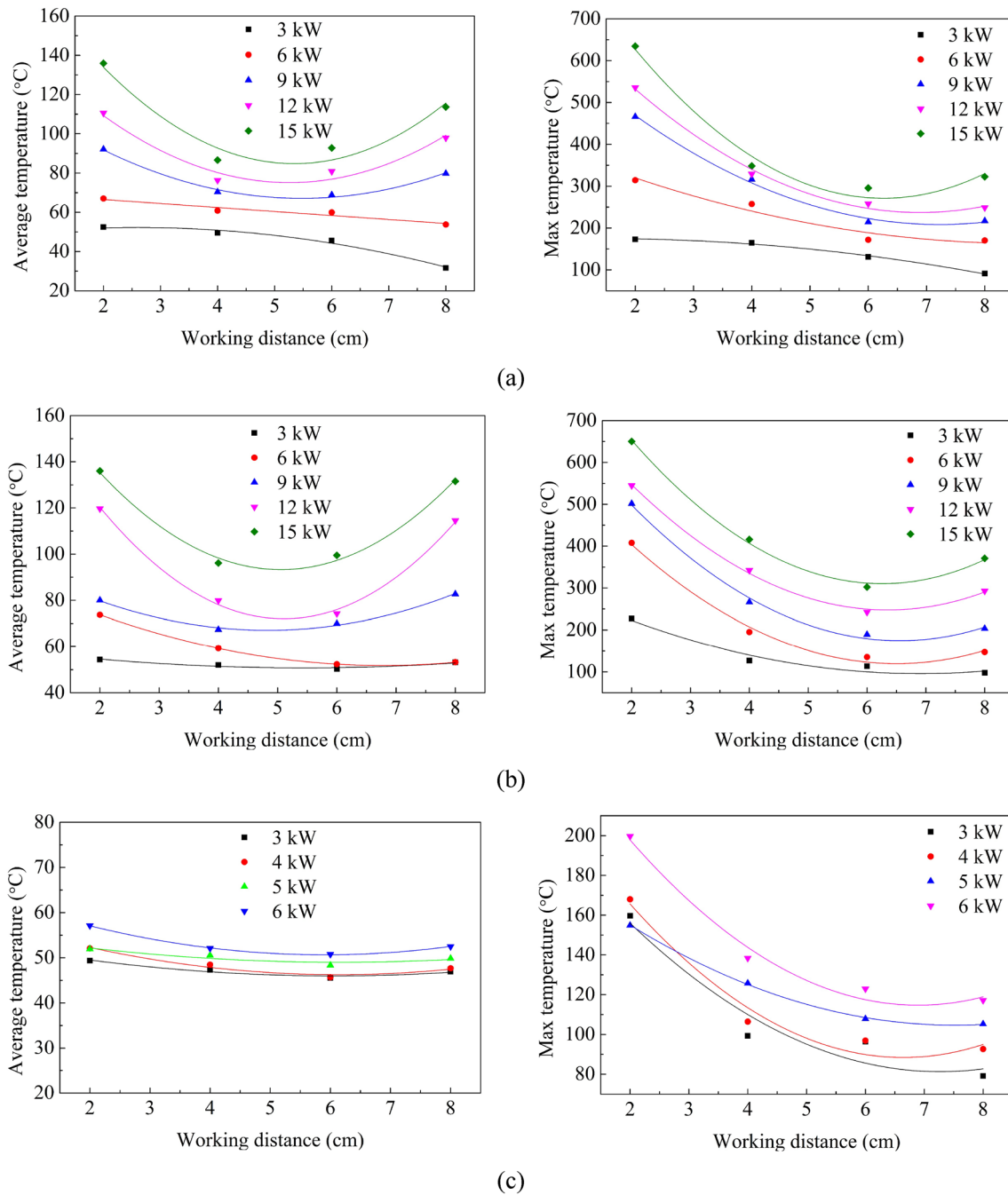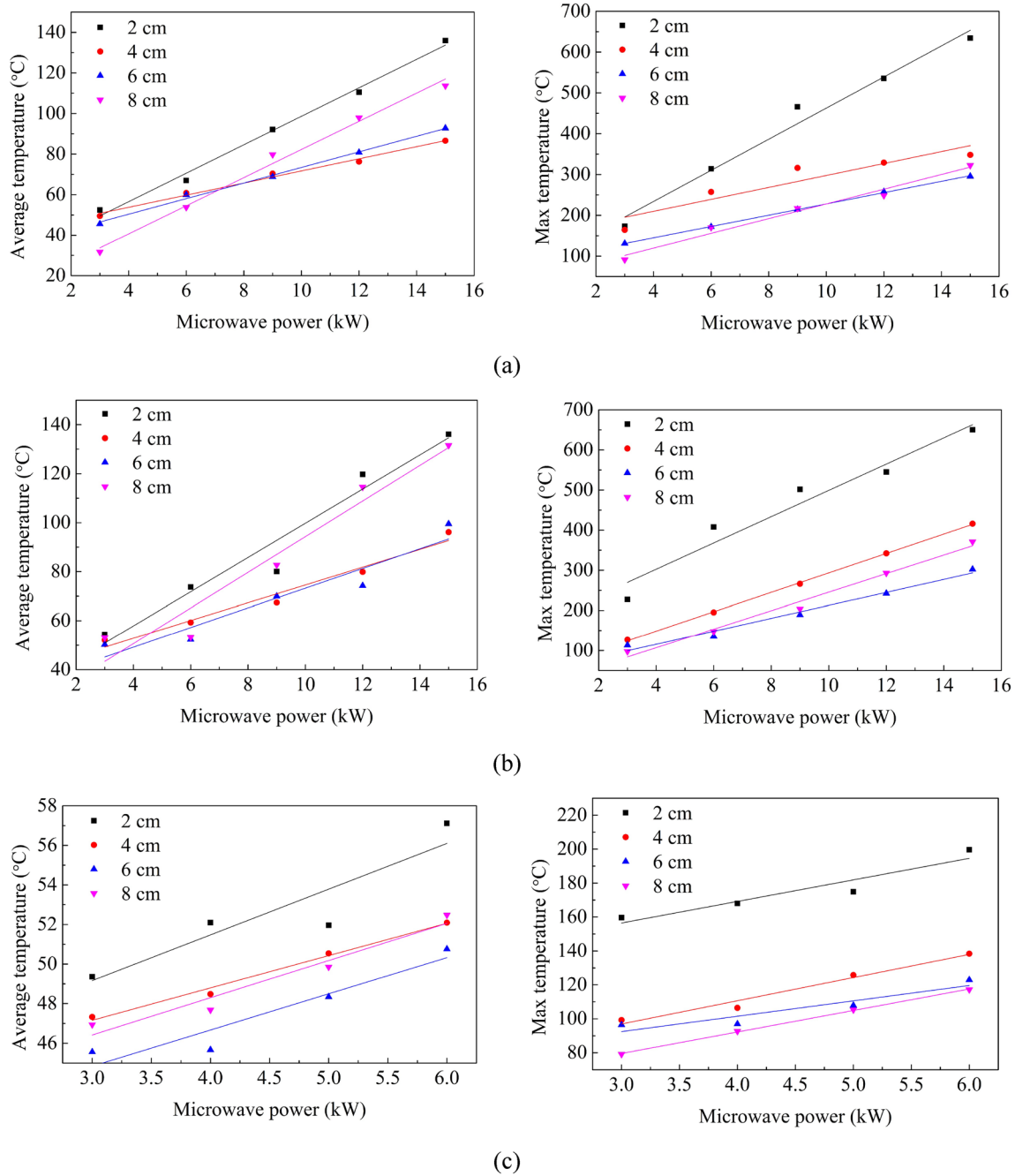
Fig. 7 Variation of the average and maximum temperatures of the irradiated surfaces of the samples with working distance for: **a** antenna 1, **b** antenna 2, and **c** antenna 3

three-dimensional surface plot (and contour plot) of the expression given in Eq. (1). The curved surface is essentially an arch that rises in the direction of increasing microwave power.

As can be seen from the above results, when the working distance is 4–6 cm, the reflection coefficient reaches the maximum and increases with the increase of power, which means that more microwave energy is reflected back to the

microwave equipment, which is obviously not conducive to the safety of the equipment. When the working distance is 2/8 cm, the reflection coefficient is minimum, which is safe for the equipment. On this basis, it is necessary to further study the microwave heating effect of the ore.

Fig. 8 Variation of the average and maximum temperatures of the irradiated surfaces of the samples with microwave power for: **a** antenna 1, **b** antenna 2, and **c** antenna 3

3.2 Temperature of the Microwave-Irradiated Samples

Figure 7 presents the temperature data recorded for the irradiated samples. As the working distance was increased, the average and maximum temperatures of the irradiated surfaces of the samples first decreased and then increased again. Also, the higher the power used, the more obvious the trend. The highest temperatures were produced when the working distance was 2 cm and the lowest values were generally produced at working distances of 4–6 cm. Also, it is noteworthy that the average surface temperatures produced when the working distance was 2 cm were similar to those produced when the working distance was 8 cm. However, the maximum temperatures produced were much higher at 2 cm compared to those at 8 cm. Under the action

of open-ended antenna, the farther away from the microwave port, the microwave power density decreases exponentially (Metaxas and Meredith 1983). Compared to 4 and 6 cm, the power density at 8 cm decreases, but the reflected power at 4 and 6 cm is greater, so this may result in more energy being absorbed at 8 cm, resulting in higher temperatures at 8 cm.

Figure 8 shows the same data plotted to highlight the variation of the temperature of the samples with microwave power. Clearly, the average and maximum temperatures of the irradiated samples increased approximately linearly with increasing microwave power. The maximum temperature produced when the working distance was 2 cm was much greater than those produced when the other three working distances were used. However, the average temperatures produced using the four working distances were relatively close.

As can be seen from Fig. 7, under the same conditions, the average and maximum temperatures of the surfaces irradiated using antenna 3 were less than those irradiated using the other two antennae. When comparing the cracking effects of different open-ended antennas, it is necessary to consider the maximum temperature and high temperature range of the rock. The higher the surface temperature, the greater the local damage. The wider the distribution of high temperature zones, the greater the overall damage (Ma et al. 2021). When other conditions (power, working distance) are the same, the temperature (maximum temperature and average temperature) of antenna 3 is much smaller than that of antenna 1 and antenna 2. In the author's previous study (Lin et al. 2022b), the microwave parameters of the first acoustic emission fracture signals under the stress-free condition of iron ore were: 15 kW, 30 s, and the working distance of

(a)

(b)

(c)
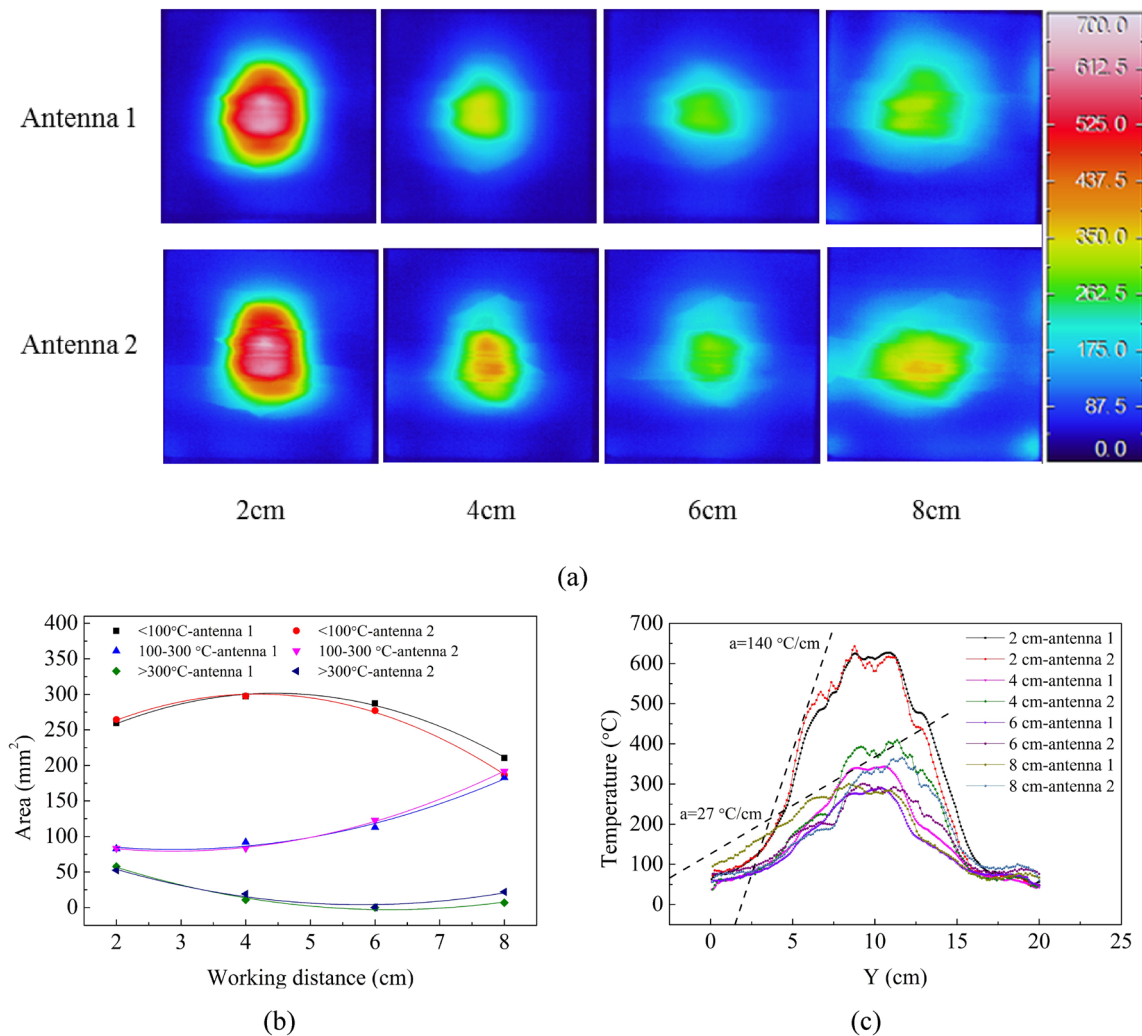
Fig. 9 Characteristics of the temperature distributions produced in the irradiated surfaces (15 kW). **a** Temperature maps of the irradiated surfaces derived from infrared images; **b** areas of the irradiated sur-

face corresponding to certain temperature ranges; **c** Temperature variation in the *Y*-direction along lines through the centers of the faces of the irradiated surfaces

6 cm. At this time, the corresponding maximum temperature is about 300 °C, with 300 °C as the boundary of the high temperature zone, and the area of the high temperature zone of antenna 3 is 0. Compared to antenna 1 and antenna 2, antenna 3 has the smallest maximum temperature and area of high temperature zone, so antenna 3 has the worst effect on cracking ore. In addition, when the power of antenna 3 is turned on to a higher level, the microwave energy is too concentrated, and an arc phenomenon occurs in the microwave antenna, resulting in a short circuit in the microwave system.

Figure 9 shows the characteristics of temperature distribution on the irradiated surface under the action of antennas 1 and 2 when the microwave power is 15 kW. Figure 9a shows the temperature distributions produced by the two antennae when the four different working distances were employed. Clearly, the temperature characteristics were very similar, including their shape, position, and area. Figure 9b shows the areas of the sample surfaces corresponding to certain temperature ranges. As can be seen, the temperature distribution characteristics produced by the two antennae were again very similar. The larger the high temperature zone (> 300 °C), the more conducive it is to expanding the cracking range, so a shorter distance is preferable.

Figure 9c shows how the temperatures of the irradiated surfaces vary across their faces (along lines passing through the centers of their irradiated faces in the Y-direction). The temperature distributions produced by the two antennae are very similar. When the working distance is 2 cm, the maximum temperature produced is over 600 °C. Moreover, as shown by the dashed line, the temperature gradient produced in the surface is as high as 140 °C/cm. In contrast, temperature gradients of just 27 °C/cm or so are produced when the antennae are further away from the ore. When a working distance of 2 cm is used, the maximum temperature and temperature gradient produced are much greater than those produced using the other working distances. Thus, a

working distance of 2 cm is highly conducive to causing damage to the ore.

In summary, our results show that antenna 3 produces the worst heating effect in the ore and much of the microwave radiation from the antenna is reflected from the sample surface. On the other hand, the reflection coefficients and heating effects (average temperature, maximum temperature, area of high temperature zone and temperature distribution) produced by antennae 1 and 2 are very similar. The essence of rock microwave cracking is that rock samples absorb microwave energy and convert it into thermal energy. The temperature difference between different minerals in the rock produces a temperature gradient. This gradient promotes the thermal expansion of minerals, resulting in deformation of mineral particles. Different deformations between mineral particles lead to different degrees of thermal stress between rock particles. Therefore, temperature gradient is an important basis for judging rock failure. Under the same microwave output conditions, high power density and short time irradiation are more conducive to rock damage, because high power and short time irradiation can produce greater temperature gradients (Whittles et al. 2003). The temperature gradient reflects the extent of local damage, and the range of high temperature zone reflects the extent of damage (Ma et al. 2021). Therefore, the heating effect is the best when the working distance is 2 cm (in which case the reflection coefficient is also rather small). From these two aspects (reflection coefficient and microwave heating effect), the best microwave parameters to use are: antenna 1 or antenna 2, a microwave power of 15 kW, and a working distance of 2 cm.

Fig. 10 Photographs of samples exposed to microwaves while subjected to true triaxial stress. **a** Exposure for 30 s using a working distance of 2 cm; **b** exposure for 300 s using a working distance of 8 cm
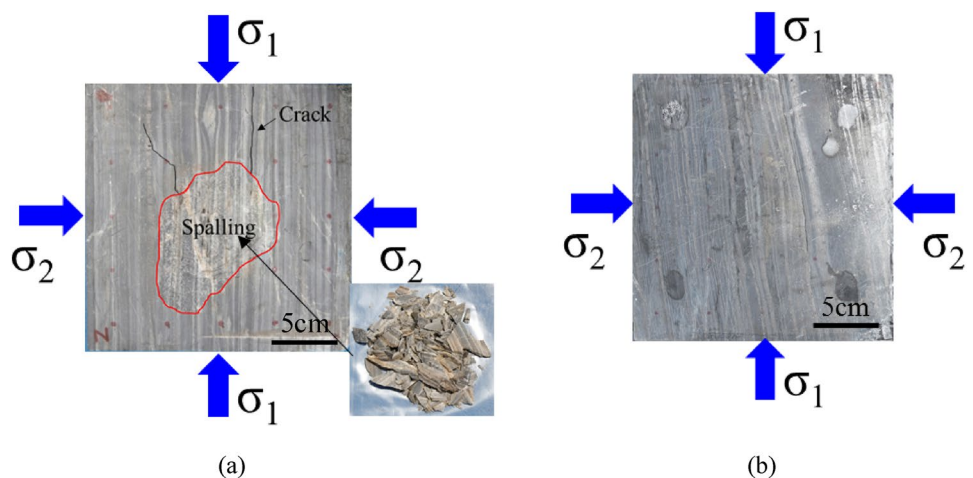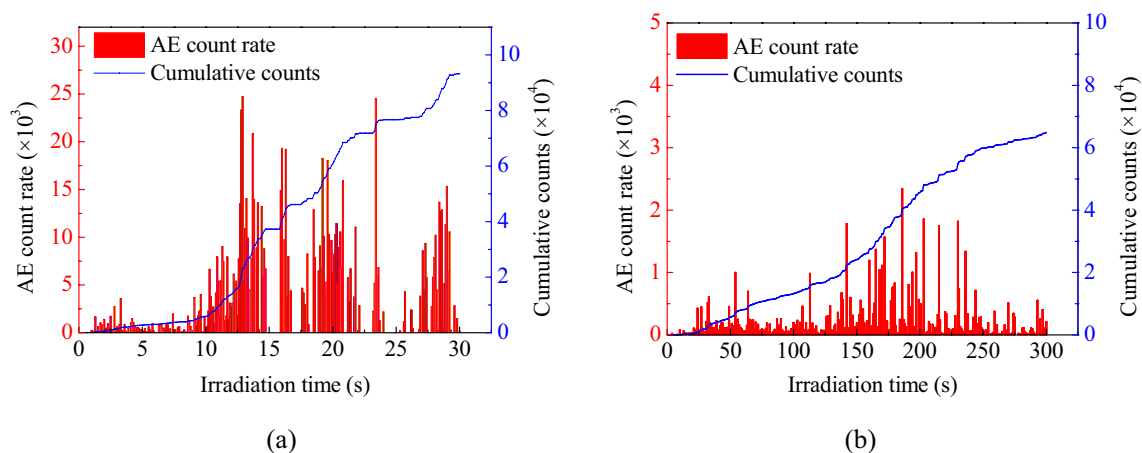
Fig. 11 Acoustic emission in samples subjected to true triaxial stress. The graphs correspond to the cases when the working distance is set to: **a** 2 cm, and **b** 8 cm

3.3 Microwave Cracking Characteristics of Samples at Different Working Distance Subjected to True Triaxial Stress

To verify the effectiveness of the abovementioned optimized parameters under true triaxial stress conditions, further microwave irradiation and cutting tests were carried out on samples under true triaxial stress. The results obtained using the optimal parameters were compared with those produced using a control group of parameters. Figure 10 shows photographs of stressed samples irradiated with microwaves using working distances of 2 cm for 30 s and 8 cm for 300 s. Clearly, much more severe damage was suffered by the sample when the working distance was 2 cm and the exposure time was short (Fig. 10a). Extensive spalling could be seen to occur when the working distance was 2 cm even though the microwave radiation (15 kW) was applied for only 30 s. The spalling in the sample caused flakes of ore to break away from the surface and scorch marks were also visible. Two large macroscopic cracks were also generated around the spalled area. Interestingly, one crack was parallel to the bedding direction and the other was at an angle of about 20° to it. In contrast, the irradiated surface of the sample shown in Fig. 10b (when the working distance was set to 8 cm) presented no macroscopic cracks even though irradiation was performed for 300 s.

3.4 Microwave Cracking Process of Samples at Different Working Distances Subjected to True Triaxial Stress

Figure 11 shows the number of acoustic emission events detected during the microwave irradiation of samples subjected to true triaxial stress. When the working distance was 2 cm (Fig. 11a), the AE activity was relatively quiet during the first 10 s of exposure to the microwaves. Thereafter, the count rate started to rise sharply. The AE activity then peaked for the first time around the 13-s mark. Alternate periods of activity and inactivity then followed which led to the cumulative AE count increasing in a ladder fashion. When the working distance was 8 cm (Fig. 11b), the AE activity in the sample also experienced quiet and active periods successively but the intensity of the AE activity was much reduced. The count rate increased sharply around the 25-s mark and peaked overall around the 180-s mark.

The AE activity in the ore was clearly much greater when a working distance of 2 cm was employed. Considering the microwave-induced cracking that occurred in the ore samples, it seemed reasonable to suggest that when the working distance was 2 cm, the energy of the sample accumulates in the first 10 s, and then forms micro cracks. The peeling (spalling) first occurred in the sample after ~ 10 s, and then occurred every few seconds. In contrast, when the working distance was 8 cm, the microwaves induced the formation of microcracks in the ore (thus producing AE) but the heating effect was not strong enough to cause these microcracks to develop sufficiently to form macroscopic cracks.

3.5 Evaluation of the Microwave-Induced Cracking Effect in the Samples

The wave velocities in the ore samples (which were measured before and after microwave irradiation) can be used to assess the cracking effect produced in the samples by the microwaves (Ma et al. 2021). Essentially, the presence of cracks slows down the propagation of waves in the ore leading to a large drop in their propagation speed. The wave velocity data were used to determine the drop in wave velocity at each of the recording points on the surfaces of the test
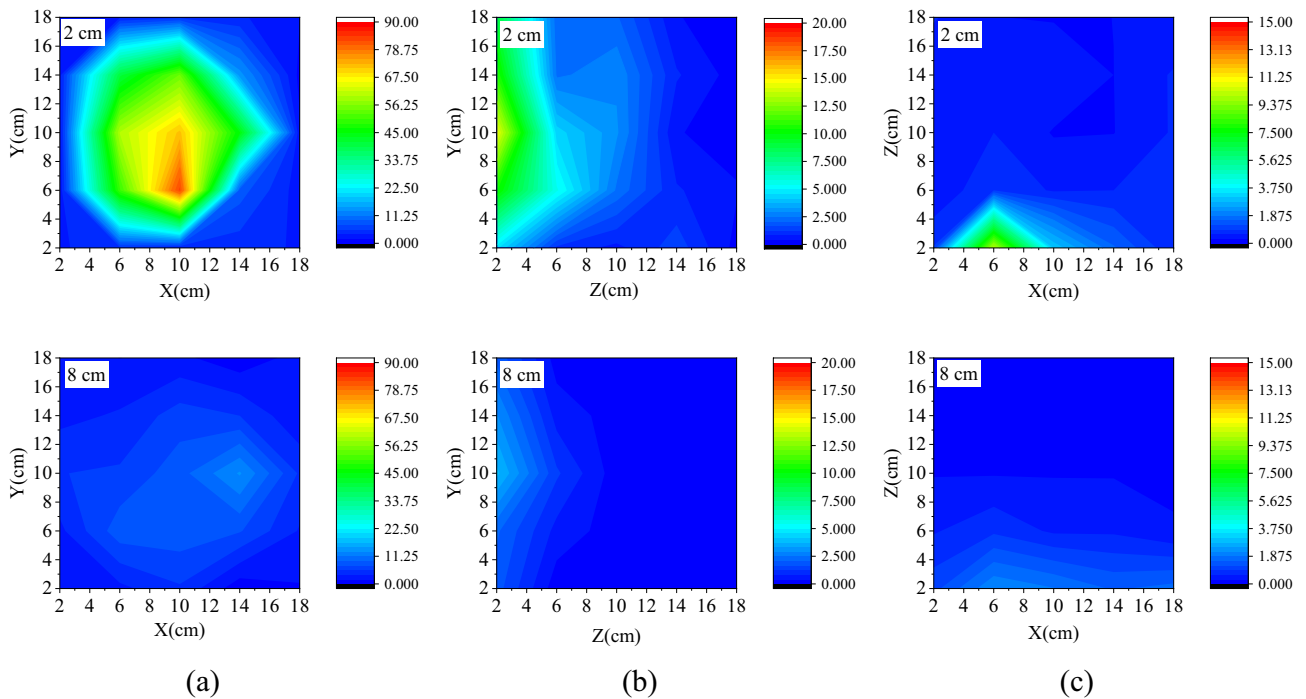
Fig. 12 Nephograms of the wave velocity drops measured in the samples along: **a** the *Z*-direction, **b** the *X*-direction, and **c** the *Y*-direction
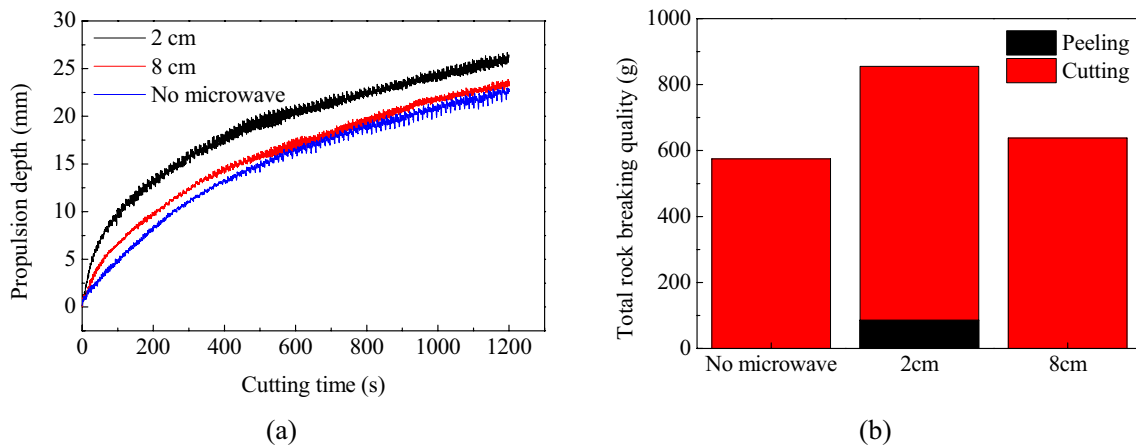
Fig. 13 Effect of working distance on cutting performance: **a** variation of propulsion depth with cutting time, and **b** total amount of broken rock collected

samples. The ratios of the wave velocity difference before and after microwave irradiation at each measuring point on the sample surface to the initial wave velocity at that point were calculated to obtain the wave velocity drop amplitude of each measuring point, and the nephogram of wave velocity drop amplitude of the sample was made (Fig. 12). In these maps, regions that are colored red represent zones in which there is a large drop amplitude in wave velocity (and blue represents no change). As already mentioned, the greater the decrease, the more severe the damage. Figure 12

implies that there is a large drop amplitude in wave velocity in the *Z*-direction when the working distance is 2 cm. Also, the corresponding drop amplitudes in the *X*- and *Y*-directions are much smaller in magnitude. The largest drop amplitude in wave velocity in the *Z*-direction is found in the center of the irradiated surface (the maxima in the *X*- and *Y*-directions are observed near to the side that is irradiated). In contrast, when the working distance is 8 cm, the drop amplitude in wave velocity is much less than that of 2 cm in all three

directions showing that much less damage (cracking) has occurred in the sample.

Mechanical cutting tests were also carried out on irradiated ore samples to evaluate the effect of the microwave treatment. Figure 13a shows how the propulsion depths in two ore samples varied with cutting time. The cutting curve when the working distance is 2 cm is clearly very steep when cutting started indicating that the cutting tool penetrated the ore easily. After rising rapidly, the slope of the curve gradually decreases and the curve is essentially linear after the 600-s mark is reached. In the absence of microwave and microwave action (working distance of 8 cm), the curve rises more stably and the initial slope is smaller. Compared with no microwave treatment, under the same propulsion time, the propulsion depth corresponding to a working distance of 2 cm is significantly improved, while the propulsion depth corresponding to a working distance of 8 cm is slightly improved.

The total amount of rock breaking off from the samples could be obtained by collecting and weighing the chippings ('peeling amount') that peeled off during the microwave irradiation process and the chippings ('cutting amount') produced during cutting. The results are shown in Fig. 13b. Compared with the samples without microwave treatment, the total rock breaking quality increased by 48.7% and 11.0% when the working distance was 2 cm and 8 cm, respectively.

4 Discussion

In the above research, it is found that under the condition of no stress, after microwave irradiation, cracks along the direction of the bedding plane appear on the ore surface. Under true triaxial stress, the surface of the ore has a remarkable spalling phenomenon. This is because the failure strength between crystals is generally smaller than that of the crystal itself. Under the condition of no stress, the microwave absorbing minerals are distributed in layers and easy to produce intergranular cracks, which expand into macroscopic cracks along the direction of the bedding plane. However, under true triaxial stress, when σ_1 is perpendicular to the bedding plane, the crack development along the bedding plane is restrained. At the same time, the combined

(a)   (b)

(c)   (d)   (e)
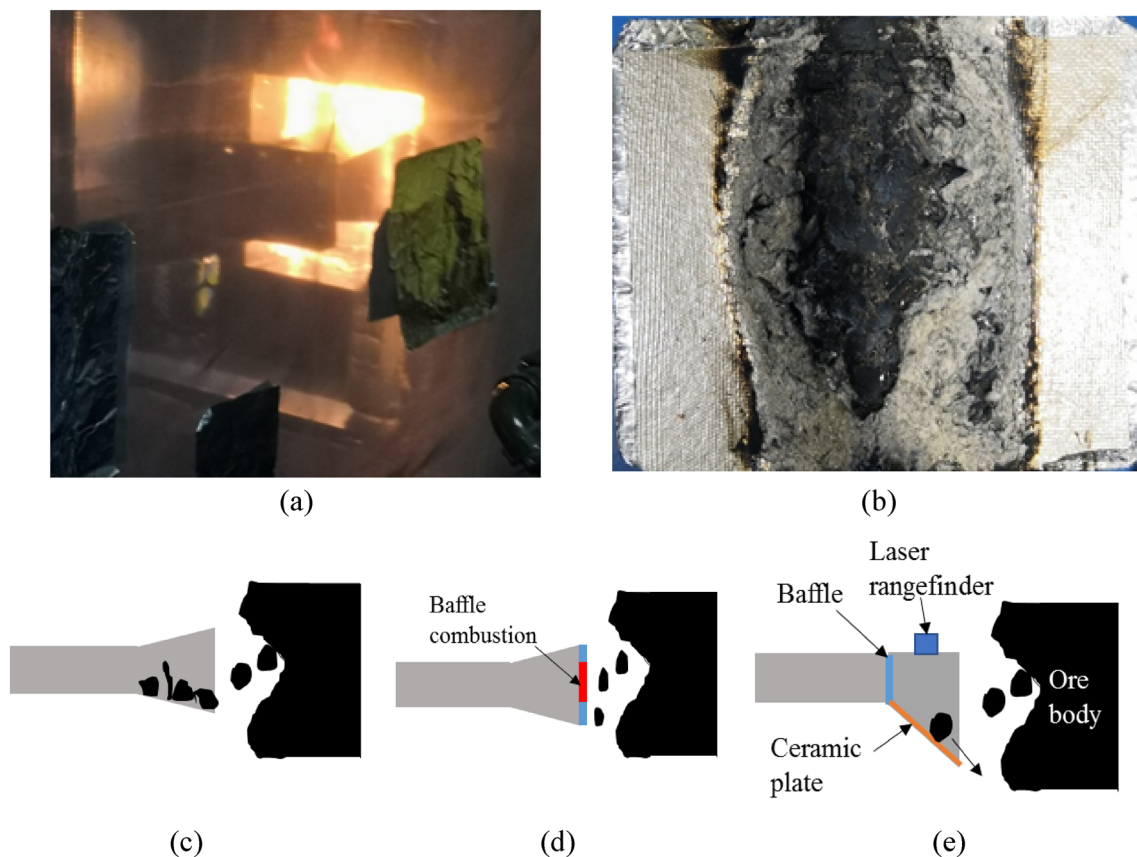
Fig. 14 Aspects of the problems associated with the antenna design: **a** The generation of electric arcing in a sample subjected to true triaxial stress; **b** a baffle burnt by the electric arcing phenomenon; **c** schematic diagram showing debris entering the antenna in the absence of a baffle; **d** schematic diagram showing hot debris burning a baffle; **e** diagram illustrating an improved antenna design

action of thermal expansion force in the Z-direction and confining pressure (σ_1 and σ_2) leads to the spalling of ore along the free surface.

The above results have shown that a good cracking effect can be induced in an ore sample subjected to true triaxial stress when the ore is irradiated by microwaves from a nearby source (i.e. the working distance used is small). Under such circumstances, the microwaves are not strongly reflected but are instead strongly absorbed. However, an interesting phenomenon occurred during our tests: arcing was found to occur when the working distance was 2 cm and the ore was subjected to true triaxial stress. This phenomenon did not occur under stress-free conditions or when larger working distances were employed. The arcing phenomenon could be reliably observed before spalling occurred. In a single test, the extent of the arcing is quite low and the baffle used is not significantly damaged. However, the baffle does become badly burnt when it is used repeatedly (Fig. 14a, b). This is because under true triaxial stress, fragments of ore flake off from the ore's surface when the sample is irradiated with microwaves and the tip generated on the ore surface will lead to arcing occurring very close to (or on) the baffle.

The function of the baffle is to prevent spalling debris from entering the antenna and accumulating (Fig. 14c) as this would clearly affect the transmission of microwaves. As the working distance is small, fragments are highly likely to make contact with the baffle and generate arcing thus causing the baffle to burn (Fig. 14d). In order to solve this problem, an improved antenna configuration is proposed, as shown in Fig. 14e. As can be seen, in this new design, the baffle is moved further away from the ore making ore–baffle contact less likely. This should prevent any arcing from directly burning the baffle. At the same time, the bottom plate of the antenna is tilted downwards so that any falling debris that enters the antenna is automatically shepherded away from the antenna preventing it from accumulating inside. Research shows that the larger the cross-sectional area of the antenna output, the more diffuse the microwave energy (Ma et al. 2021). Therefore, if the horn of the antenna is equiangular, tilting the bottom plate of the antenna will lead to the antenna output having a larger cross-sectional area. Thus, the new design uses a right-angled horn to ensure that the cross-sectional area of the antenna output is not increased significantly. The ceramic plate in the new antenna does not absorb the microwaves and has a high temperature resistance (melting point above 2000 °C). Thus, it will help prevent damage being caused to the antenna by hot debris fragments ejected from the ore.

In normal operation in the field, the working face of the ore will not be completely flat. Therefore, there is a danger

Table 3 Ore parameters used in the numerical simulations

Relative permittivity	Loss factor	Specific heat (J/kg°C)	Density (kg/m³)	Electrical conductivity (S/m)	Thermal conductivity (W/mK)
18.1	0.5	800	3000	10	7.5

(a)   (b)
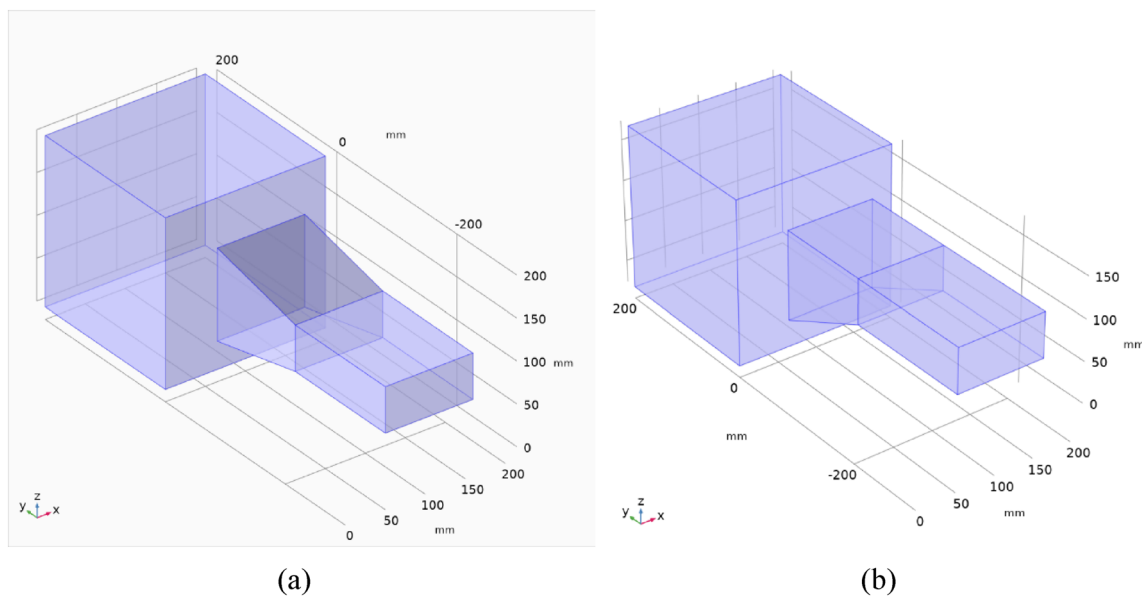
Fig. 15 Geometric models of the antennae used in the numerical simulations: **a** antenna with an equiangular horn, and **b** antenna with a right-angled horn

that the antenna could easily collide with the working face as the working distance is required to be small to maximize the efficiency of the irradiation process. To help overcome this problem, a laser rangefinder can be attached to the antenna to precisely control the distance between the output end of the antenna and the working face of the ore, thus maintaining the correct (optimum) working distance.

The proposed antenna design still has some issues that need to be considered further: (i) If a working distance of 2 cm is used, will debris become trapped between the antenna and the working face of the ore? (ii) How much should the bottom plate of the antenna be inclined to ensure that the debris slides away from the antenna? (iii) Does the change in the structure of the antenna weaken the microwave-induced degradation effect in the ore?

To help address some of these issues, first, some peeled ore debris was placed in an antenna and lifted one end of the antenna until the debris inside slid freely. The critical inclination angle was found to be about 24°. Furthermore, a gap of 2 cm was present (to reproduce the optimum working distance) and it was found that the ore debris was able to fall normally without becoming jammed. COMSOL software was then used to simulate the irradiation of ore samples using an equiangular vs. a right-angled horn antenna. The geometric models are shown in Fig. 15. The design was based on a WR430 transmission waveguide which employs a section width of 109.22 mm and

height of 54.61 mm. The transmission waveguide was connected to the antenna horn and a sample of ore (measuring 200 mm×200 mm×200 mm) was placed 2 cm in front of the output end of the antenna horn. The parameters used to simulate the ore are presented in Table 3.

The transmission waveguide and antenna surfaces were assigned the properties of copper and the interior and exterior regions were set to air. The output ends of both antennae were set to 109.22 mm×109.22 mm. The angles of inclination of the bottom plates were taken to be equal to 12.7° (equiangular horn antenna) and 24° (right-angled horn antenna). The thermal convection coefficient was taken to be 20 W/(m^2 °C), the microwave power was set to 15 kW, and the irradiation time was set to 30 s.

Figure 16 shows the surface temperature distributions produced in the samples after microwave irradiation. As can be seen, the two temperature distributions are essentially the same. The average (maximum) temperature of the irradiated surface in Fig. 16a is 157.3 °C (916.7 °C). The average (maximum) temperature in Fig. 16b is 156.4 °C (885.0 °C). Therefore, the microwave irradiation effect achieved in the ore using the right-angled horn antenna is not significantly weakened compared to the equiangular design. Moreover, the angle of inclination of the bottom plate is larger in the former, which is much better for removing debris.

(a)　　　　　　　　　　　　　　　　　　　　　　　(b)
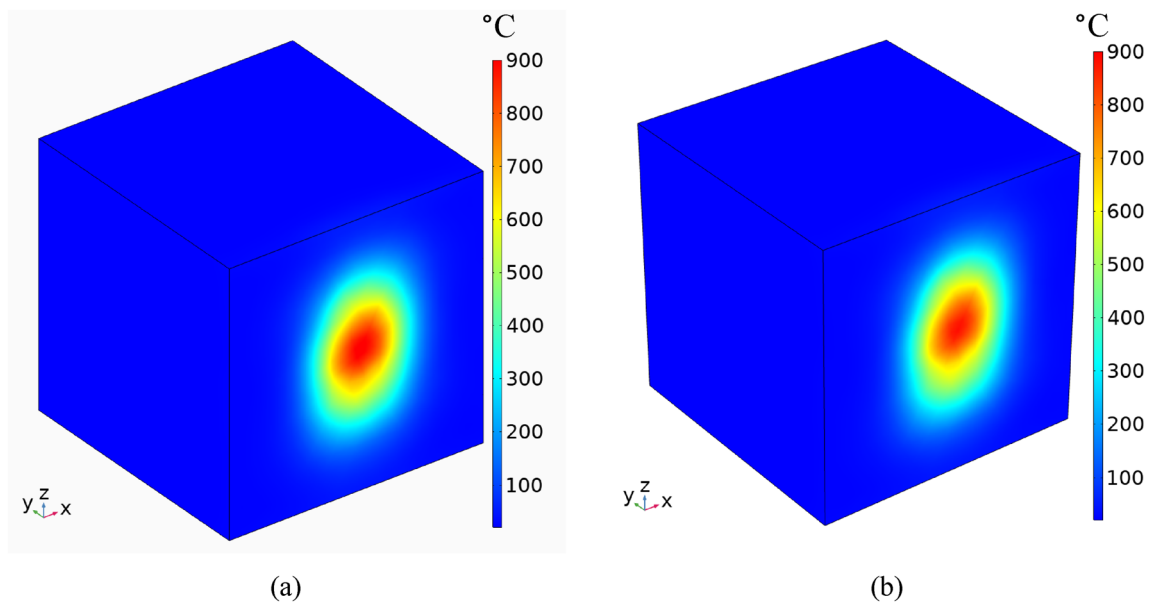
Fig. 16 Surface temperature distributions produced after irradiating samples with microwaves using: **a** the equiangular horn antenna, and **b** the right-angled horn antenna

5 Conclusion

The effects of varying various microwave parameters (antenna type, working distance, and microwave power) on unstressed samples of Sishanling iron ore were first investigated in this work. The study focuses on the reflectivity of the ore and temperature changes induced by the microwaves. The optimum values of the microwave parameters were thus obtained. Microwave irradiation and mechanical cutting tests were then carried out using ore subjected to true triaxial stress to verify the effectiveness of the parameters derived. Finally, the optimization of the antenna was also discussed. The results show that:

1. As the working distance is increased (2–8 cm), the reflection coefficient of the ore increases, peaks, and then decreases again. The peak value appears around 4–6 cm. For antenna 1 and antenna 2, the reflection coefficient is basically the same at working distances of 2 cm and 8 cm. The reflection coefficient also increases linearly as the microwave power is increased. When all other conditions were the same, antenna 3 produced the largest reflection coefficients; those produced by antennae 1 and 2 were very similar.

2. Regardless of which antenna was used, the average and maximum temperature produced in the irradiated surface of the samples first decreased and then increased again as the working distance was increased. A working distance of 2 cm produced the highest temperatures and temperature gradients. The temperature of the irradiated surface was found to increase approximately linearly with increasing microwave power. The average and maximum temperatures produced using antenna 3 were less than those produced using the other two antennae. The temperature distributions and gradients produced using antennae 1 and 2 were essentially the same.

3. Using a working distance of 8 cm, samples subjected to true triaxial stress exhibited no macroscopic signs of damage even when irradiated for 300 s. When the working distance was reduced to 2 cm, however, the samples started to break up after just 10 s. The ore failed via a series of intermittent spalling events. Compared with the samples without microwave treatment, the total rock breaking quality increased by 48.7% and 11.0% when the working distance was 2 cm and 8 cm, respectively.

4. Irradiated samples subjected to true triaxial stress were prone to arcing when the working distance was 2 cm. When this happened the baffle of the antenna could catch fire. An optimized antenna was proposed to overcome this problem and the effectiveness of the optimized design verified via numerical simulation.

Declarations

Conflict of interest The authors declare that they have no conflicts of interest.

References

Amankwah RK, Khan AU, Pickles CA, Yen WT (2005) Improved grindability and gold liberation by microwave pretreatment of a free-milling gold ore. Min Proc Ext Met 114(1):30–36. https://doi.org/10.1179/037195505X28447

Armaghani DJ, Yagiz S, Mohamad ET, Zhou J (2021) Prediction of TBM performance in fresh through weathered granite using empirical and statistical approaches. Tunn Undergr Sp Technol 118:104183. https://doi.org/10.1016/j.tust.2021.104183

Ciccu R, Grosso B (2014) Improvement of disc cutter performance by water jet assistance. Rock Mech Rock Eng 47:733–744. https://doi.org/10.1007/s00603-013-0433-4

Deyab SM, Rafezi H, Hassani F, Kermani M, Sasmito AP (2021) Experimental investigation on the effects of microwave irradiation on kimberlite and granite rocks. J Rock Mech Geotech Eng 13(2):267–274. https://doi.org/10.1016/j.jrmge.2020.09.001

Entacher M, Lorenz S, Galler R (2014) Tunnel boring machine performance prediction with scaled rock cutting tests. Int J Rock Mech Min Sci 70:450–459. https://doi.org/10.1016/j.ijrmms.2014.04.021

Feng XT, Zhang JY, Yang CX, Tian J, Lin F, Li SP, Su XX (2021) A novel true triaxial test system for microwave-induced fracturing of hard rocks. J Rock Mech Geotech Eng 13:961–971. https://doi.org/10.1016/j.jrmge.2021.03.008

Feng XT, Su XX, Yang CX, Lin F, Li SP, Zhang JY, Tong TY (2022) A test system for microwave-assisted dual-mode mechanical cutting hard rock under true triaxial compression. Rock Mech and Rock Eng **(under review)**

Haque KE (1999) Microwave energy for mineral treatment processes. Int J Miner Process 57(1):1–24. https://doi.org/10.1016/s0301-7516(99)00009-5

Hartlieb P, Grafe B (2017) Experimental study on microwave assisted hard rock cutting of granite. BHM Berg-Huettenmaenn Monatsh 162(2):77–81. https://doi.org/10.1007/s00501-016-0569-0

Hartlieb P, Grafe B, Shepel T, Malovyk A, Akbari B (2017) Experimental study on artificially induced crack patterns and their consequences on mechanical excavation processes. Int J Rock Mech Min Sci 100:160–169. https://doi.org/10.1016/j.ijrmms.2017.10.024

Hassani F, Nekoovaght P (2011) The development of microwave assisted machineries to break hard rocks. In: Proceedings of the 28th international symposium on automation and robotics in construction (ISARC), Seoul, South Korea. https://doi.org/10.22260/isarc2011/0127

Hassani F, Nekoovaght PM, Gharib N (2016) The influence of microwave irradiation on rocks for microwave-assisted underground excavation. J Rock Mech Geotech Eng 8:1–15. https://doi.org/10.1016/j.jrmge.2015.10.004

Hassani F, Shadi A, Rafezi H, Sasmito AP, Ghoreishi-Madiseh SA (2020) Energy analysis of the effectiveness of microwave-assisted fragmentation. Miner Eng 159:106642. https://doi.org/10.1016/j.mineng.2020.106642

Huang J, Xu G, Hu G, Kizil M, Chen Z (2018) A coupled electromagnetic irradiation, heat and mass transfer model for microwave heating and its numerical simulation on coal. Fuel Process Technol 177:237–245. https://doi.org/10.1016/j.fuproc.2018.04.034

Jerby E, Dikhtyar D, Aktushev O, Grosglick U (2002) The microwave drill. Science 298:587–589. https://doi.org/10.1126/science.1077062

Kahraman S, Canpolat AN, Fener M (2020) The influence of microwave treatment on the compressive and tensile strength of igneous rocks. Int J Rock Mech Min Sci 129:104303. https://doi.org/10.1016/j.ijrmms.2020.104303

Kingman SW, Corfield GM, Rowson NA (1999) Effects of microwave radiation upon the mineralogy and magnetic processing of a massive Norwegian ilmenite ore. Magnet Elect Separ 9:131–148. https://doi.org/10.1155/1999/57075

Kingman SW, Vorster W, Rowson NA (2000) The influence of mineralogy on microwave assisted grinding. Miner Eng 13(3):313–327. https://doi.org/10.1016/S0892-6875(00)00010-8

Kingman SW, Jackson K, Bradshaw SM, Rowson NA, Greenwood R (2004) An investigation into the influence of microwave treatment on mineral ore comminution. Powder Technol 146(3):176–184. https://doi.org/10.1016/j.powtec.2004.08.006

Lester E, Kingman SW (2004) Effect of microwave heating on the physical and petrographic characteristics of a UK coal. Energ Fuel 18:140–147. https://doi.org/10.1021/ef030088c

Lin F, Feng XT, Lu GM, Su XX, Li SP, Zhang JY (2021) Study on microwave heating order and electromagnetic characteristics of copper and gold ores. Rock Mech Rock Eng 54(5):2129–2143. https://doi.org/10.1007/s00603-021-02376-4

Lin F, Feng XT, Yang CX, Li SP, Zhang JY, Su XX, Tong TY (2022a) Microwave response characteristics and influencing factors of ores based on dielectric properties of synthetic samples. J Rock Mech Geotech Eng 14(2):315–328. https://doi.org/10.1016/j.jrmge.2021.08.002

Lin F, Feng XT, Yang CX, Li SP, Zhang JY, Su XX, Tong TY (2022b) Experimental study on improving mechanical mining efficiency of deep banded iron ore by microwave presplitting. Int J Rock Mech Min Sci 159:105233. https://doi.org/10.1016/j.ijrmms.2022.105233

Liu P, Liang WH (2000) Design considerations for construction of the Qinling Tunnel using TBM. Tunn Undergr Sp Technol 15:139–146. https://doi.org/10.1016/S0886-7798(00)00041-9

Lu GM, Feng XT, Li YH, Zhang XW (2019) The microwave-induced fracturing of hard rock. Rock Mech Rock Eng 52:3017–3032. https://doi.org/10.1007/s00603-019-01790-z

Ma ZJ, Zheng YL, Li XZ, Zhao XB, He L, Zhao QH, He JL, Li JC (2021) Design and performance of an open-ended converging microwave antenna in fracturing biotite diorite at low microwave power levels. Geomech Geophys Geo-Energy GeoResour 7(4):95. https://doi.org/10.1007/s40948-021-00291-0

Ma ZJ, Zheng YL, Li JC, Zhao XB, Zhao QH, He JL, Fu HY (2022) Characterizing thermal damage of diorite treated by an open-ended microwave antenna. Int J Rock Mech Min Sci 149:104996. https://doi.org/10.1016/j.ijrmms.2021.104996

Maurer W (1968) Novel drilling techniques. Pergamon Press, London

Metaxas AC, Meredith RJ (1983) Industrial microwave heating. Peter Peregrinus Ltd., London

Montross CS, Florea V, Bolger JA (1999) Laser-induced shock wave generation and shock wave enhancement in basalt. Int J Rock Mech Min Sci 36(6):849–855. https://doi.org/10.1016/s0148-9062(99)00054-6

Natanzi AS, Laefer DF (2015) Using chemicals as demolition agents near historic structures. In: 9th International conference on structural analysis of historical constructions, Mexico City, Mexico. http://researchrepository.ucd.ie/handle/10197/6798

Peinsitt T, Kuchar F, Hartlieb P, Moser P, Kargl H, Restner U, Sifferlinger N (2010) Microwave heating of dry and water saturated basalt, granite and sandstone. Int J Min Miner Eng 2(1):18–29. https://doi.org/10.1504/ijmme.2010.031810

Rostami J (2016) Performance prediction of hard rock Tunnel Boring Machines (TBMs) in difficult ground. Tunn Undergr Sp Technol 57:173–182. https://doi.org/10.1016/j.tust.2016.01.009

Shepel T, Grafe B, Hartlieb P, Drebenstedt C, Malovyk A (2018) Evaluation of cutting forces in granite treated with microwaves on the basis of multiple linear regression analysis. Int J Rock Mech Min Sci 107:69–74. https://doi.org/10.1016/j.ijrmms.2018.04.043

Teimoori K, Cooper R (2021) Multiphysics study of microwave irradiation effects on rock breakage system. Int J Rock Mech Min Sci 140:104586. https://doi.org/10.1016/j.ijrmms.2020.104586

Toifl M, Meisels R, Hartlieb P, Kuchar F, Antretter T (2015) 3D numerical study on microwave induced stresses in inhomogeneous hard rocks. Miner Eng 90:29–42. https://doi.org/10.1016/j.mineng.2016.01.001

Whittles DN, Kingman SW, Reddish DJ (2003) Application of numerical modelling for prediction of the influence of power density on microwave-assisted breakage. Int J Miner Process 68(1):71–91. https://doi.org/10.1016/S0301-7516(02)00049-2

Zheng YL, Zhang QB, Zhao J (2017) Effect of microwave treatment on thermal and ultrasonic properties of gabbro. Appl Therm Eng 127:359–369. https://doi.org/10.1016/j.applthermaleng.2017.08.060

Zheng YL, Ma Z, Zhao X, He L (2020) Experimental investigation on the thermal, mechanical and cracking behaviours of three igneous rocks under microwave treatment. Rock Mech and Rock Eng 53(8):3657–3671. https://doi.org/10.1007/s00603-020-02135-x